Application and Modeling of a Magnetic WSN for Target Localization

Sajjad Baghaee
Dept. of Electrical and Electronics Eng.
Middle East Technical University
Ankara, Turkey
sajjad@baghaee.com

Sevgi Zubeyde Gurbuz
Dept. of EE, TOBB ETU
and TUBITAK UZAY
Ankara, Turkey
szgurbuz@etu.edu.tr

Elif Uysal-Biyikoglu
Dept. of Electrical and Electronics Eng.
Middle East Technical University
Ankara, Turkey
elif@eee.metu.edu.tr

***Abstract*—The aim of this study is modeling ferromagnetic targets for localization and identification of such objects by a wireless sensor network (WSN). MICAz motes were used for setting up a wireless sensor network utilizing a centralized tree-based system. The detection and tracking of ferromagnetic objects is an important application of WSNs. This research focuses on analyzing the sensing limitations of magnetic sensors via tests conducted on small-scale targets which are moving within a 30 cm radius around the sensors. To detect target pres-ence and determine direction of motion, changes in magnetic field intensity are measured by the magnetic sensors. Target detection, identification and sequential localization (DISL) were accomplished using a minimum distance algorithm. The effect of environmental variations, such as temperature and power supply variations and magnetic noise, on DISL performance is examined based on experimental tests.**

Keywords- Wireless Sensor Network (WSN); Magnetic Sensor; Identification; Localization; Sequential Localization; OMP

I. INTRODUCTION

Nowadays distributed wireless sensor networks (WSN) have been widely used for a variety of military and civilian applications to monitor physical and environmental conditions. A common use of WSNs is detecting, classifying or identifying, localizing and tracking one or more objects in WSN coverage. For example, WSNs have been proposed for the estimation of road traffic patterns and traffic measurement, object detection schemes [1], [2] and intelligent traffic guidance systems [3], [4]. In particular, object classification was done by magnetic sensors in [2], [5], [6]. In these studies target identification is based on magnetic signatures of the ferromagnetic objects. Multiple targets tracking, detection and classification on the airport surfaces is discussed in [7]. In all of the reported literature, large ferromagnetic objects, such as cars and airplanes are used as a target for detection, tracking and classification. In this research, detection, identification, and sequential localization is done for small ferromagnetic targets, such as iron bars, rather than vehicles or airplanes, so that detailed tests on sensing limitations could be conducted in a laboratory environment, to aid in developing more precise models for the response of these sensors. A key question addressed in this work is with what resolution a ferromagnetic target may be detected and localized.

In previous work [8], localization of a target was done via least-squares estimation. This estimator chooses the parameter vector P such that the difference between the magnetic signal model data and measurements is minimized. In [8] the global optimization problem was solved using simulated annealing [9]. However, this technique cannot be generalized to multiple target localization. This paper explores the use of a minimum distance technique, orthogonal matching pursuit (OMP) [10], which permits incorporation of the multi-target situation as well as feature extraction for target identification. OMP has been used in other applications such as signal recovery [11], [12], radar-based human detection [13], and the detection and location estimation of a metal target underground [14]. For prolonging the network lifetime, energy consumption minimization in each node must be considered. In [15], [16], [17], [18] sensor sleep state management techniques have been proposed. In this regard, the more information that is obtained about target movements, the better the network can be managed for energy savings. Thus, developing signal processing algorithms that could permit the extraction of target location, rather than just proximity to sensor, is important. Typically, the RF communication area (sensing area) of wireless sensor nodes is wider than monitoring area. This kind of overlapping of sensing regain may increase the detection / estimation performance, but in terms of economic communication this will increase the amount of the total energy consumption in the network. On the other hand, when the sensors distributed sparsely - no sensing region overlapping - fewer sensors are used for covering an area, so the cost of network will decrease significantly. However, target tracking performance should be improved by increasing the information about the target extracted from each sensor measurement. For this study we implemented a sparse network. In this form of sensor distribution, there are gaps between the sensing area of the sensors, which we call blind zones. In blind spots, target detection is impossible and the collected data while the target are in these regions cannot guarantee the reliability of any variations in the monitored region sufficiently. Sparseness is a reality in many WSN scenarios where the sensing radii of sensors are smaller (often, an order of magnitude smaller) than communication radii, and a cost-effective implementation precludes increasing sensor density. Yet, to minimize the area of blind spots in our implementation, the sensors were spread on the

area such that they will have minimum sensing region intersection with adjacent sensor sensing region. When a target enters the sensing region of a sensor, that sensor can broadcast a message which contains the location of that target. This message can be used to set distant sensor nodes to sleep mode and save their energy, consequently. This method we can increase the lifetime of the network. Energy efficient design is one of the underlying themes of this work.

The outline of the rest of the paper is as follows. Section II introduces the abbreviations and notation to be used throughout the paper. Descriptions of the system architecture and target characteristics, development of target models and related magnetometer measurements are presented in Section III. Section IV includes the definition of the OMP algorithm and usage of OMP for localization and classification of a target in WSN. Section V presents the results validating performance of DISL system and Section VI shows the impact of environmental factors on measurements in implementing magnetic WSN and Finally, Section VII discusses future work and conclusions.

II. ABBREVIATIONS

As defined earlier, OMP expresses a greedy algorithm which is short form of the Orthogonal Matching Pursuit. Each entry of the OMP dictionary is named atom. We shall refer to the MIB520 USB interface board which connected to a laptop PC as the base station. The abbreviation DISL system refers to the combination of wireless magnetic sensors, base station and the algorithm (OMP). DISL is short form for detection, identification, and sequential localization.

III. SYSTEM ARCHITECTURE

A. Overview

The DISL system can be broken down to :

- Distributed magnetic sensors, sense and obtain the variations of the magnetic field and transmit the data wirelessly to the basestation.
- The base-station receives data from the sensors and processes them.
- The software which basically runs the OMP algorithm produces visual input on detected changes in the sensing zone.

In the following, we explain the features of the hardware, software and the algorithm of the DISL system.

B. Hardware

Our testbed (Figure.1.a) employs MICAz motes equipped with MTS310CB [19] sensor boards, a gateway MICAz mote with a MIB520 programming board from Crossbow Technology, and a PC acting as the fusion center. Each MICAz mote is equipped with an IEEE 802.15.4 compliant, Chipcon CC240 RF transceiver and Atmega 128L microcontroller. The MTS310CB sensor board includes a Honeywell HMC1002 2-axis magnetometer [20].

(a) TestBed (b) Targets 1-3 (c) Target 4

Figure 1. DISL system.

C. Software

To program the MICAz motes, the open-source operating system TinyOS-2.1.0 was used [22]. A centralized tree-based network was established using the Collection Tree Protocol (CTP) [21] implemented by the TinyOS Network Protocol Working Group (Net2WG). TinyOs 2.1.0 was installed and applied for MICAz mots programing in our network. For generating and modifying the codes, Eclipse IDE v3.5.0 which is equipped with Yeti2 plugin (a TinyOS plugin) was used. Data processing for DISL was done in MATLAB.

D. Target Characteristics

The four target configurations used are as follows:

- 1: an iron bar 15 cm long and 3 cm in diameter;
- 2: an iron bar 30 cm long and 3 cm in diameter;
- 3: an iron bar 30 cm long with a cubic cross section of 3 × 3 cm;
- 4: the combination of two iron bars, targets 1 and 3 taped together.

Targets 1, 2 and 3 are made from a homogeneous alloy. The shapes of these targets are different but symmetric (Figure 1.b). On the other hand, target number 4 is a non-homogeneous and non- symmetric target (Figure 1.c); composed of different ferromagnetic materials.

E. Target modeling

Modeling the magnetic field intensity produced for various relative locations of a sensor and a target, various directions of motion, etc. are essential for successful use of these sensors in our system, thus comprise a central piece of this work. Basically, a ferromagnetic object induces a change in the magnetic field intensity in its surroundings. This field depends on magnetic properties of that ferromagnetic object. Figure 2, illustrates the disturbance generated by a ferromagnetic object in the Earth's uniform magnetic field. The magnetic field of these targets when tested in the laboratory matched well with a dipole model [23] [8], a model widely used in the literature for many different types of targets, ranging from cars to humans [24]. This model is formulated as follows. This equation shows the magnetic field (B) of a point dipole moment *m* at distance *r* from ferromagnetic object:

$$\vec{B}(\vec{r}) = \frac{\mu_0}{4\pi}\frac{1}{r^3}\left(3(m.\vec{r})\vec{r} - m\right) = \frac{\mu_0}{4\pi}\left(\frac{3(\vec{m}\cdot\vec{r})\vec{r}}{\|\vec{r}\|^5} - \frac{\vec{m}}{\|\vec{r}\|^3}\right) \quad (1)$$

Figure 2. Effect of Ferrous object on Earth's magnetic field.

- μ_0 is the permeability of vacuum.
- r is L-2 norm of the vector $\vec{r}$
- $\bar{r}$ is the unit vector in r direction.
- m is magnetic moment.

F. Software

The Honeywell HMC1002 magnetometer is comprised of two Wheatstone bridges in two orthogonal directions. Any change in the magnetic field triggers a change in resistance, which is in turn reflected as a change in voltage across the Wheatstone bridge that is converted to a 1024 bit reading by the MICAz's analog to digital converter (ADC) circuit. This ADC reading may be derived in terms of the applied magnetics flux. First, the differential output voltage, Vdiff, is expressed in terms of the applied magnetics flux, B_s [25]:

$$V_{diff} = S \times V_b \times B_S + V_{offset} \tag{2}$$

where S is the sensitivity (mV/V/Gauss), V_b is the bridge supply voltage (V), and V_{offset} is the bridge offset voltage (mV). According to the HMC1002 data sheet [20], the sensor sensitivity varies between 2.5 and 4 mV/V/Gauss. For finding sensitivity value of a magnetic sensor, several methods have been suggested in [26].

The differential output voltage Vdiff is mapped to the full span of the ADC by amplifying Vdiff over two stages and then using a voltage-divider potentiometer to ensure the output remains within the limits of the ADC. So, the gain for each amplifier stage is given as [27]

$$G_1 = 5 + \frac{80K\Omega}{R_{G1}} = 5 + \frac{80K\Omega}{3.3K\Omega} = 29.242 \tag{3}$$

$$G_2 = 5 + \frac{80K\Omega}{R_{G2}} = 5 + \frac{80K\Omega}{1.1K\Omega} = 77.727 \tag{4}$$

Here, R_{G1} and R_{G2} are the external resistors on the magnetometer circuit used to adjust the gain of each amplifier. If V_{AB} = 0.5282 V is the maximum possible voltage difference across the potentiometer, then the voltage difference at the input of the ADC is:

$$V_{ADC} = \frac{V_{AD}}{256} \times G_2 = 2.0633 \times 77.727 = 160.37mV. \tag{5}$$

The full-scale ADC output is 210-1=1023 for a 3 V supply,

$$\frac{V_{ADC} \times 1023}{3000} \cong 54ADC \tag{6}$$

Thus, one unit of change in the potentiometer value offsets the ADC reading by 54 ADC counts, a result that was also experimentally verified. The actual magnetic sensor reading can be calculated by offsetting the ADC reading by the change in ADC units due to the PotentiometerBias(PB).

$$ADC_{total} = ADC + 54 \times PB \tag{7}$$

and converting the units to Gauss to obtain

$$V_{diff} \times G_{total} \times \frac{ADC_{fullscale}}{V_{\sup}} = ADC_{total} \tag{8}$$

Here, G_{total} is computed as $G_1 \times G_2$= 29 × 78 = 2262. The measured magnetic field for either magnetometer axis may then be found to be

$$B_S = \frac{(ADC + 54 \times PB)}{0.001 \times G_{total} \times ADC_{fullscale} \times S} - \frac{V_{offset}}{V_b \times S} \tag{9}$$

IV. THE A LGORITHM

A. OMP overview

For this study an iterative greedy algorithm which is called Orthogonal Matching Pursuit (OMP) [10] is used. OMP is a sparse approximation technique such as "basis pursuit" [28] a "matching pursuit" [29]. OMP tries to find the "best match" (minimum distance) projections of multidimensional data onto an over-complete dictionary D with a predefined number of iterations. In each iteration, a column of dictionary D which has maximum correlation with that iteration's residual r is selected. This locally optimum solution is recorded as ith element of the coefficient vector C where the i shows the step (iteration) number. In order to use OMP algorithm we need a dictionary which is created by using signal parametric model. We divided the sensing region of each sensor to 28 sub-regions and 4 sub-regions and obtain data from each point for generating a dictionary. This procedure will be discussed in greater in subsequent sections. The goal is to recover the tested signal can by combination of correct items (γ) in a minimum number of iterations, where the estimate after the η^{th} iteration is as follows:

$$\hat{S} = \sum_{j=1}^{J} C_j . \hat{\gamma}(\xi_\eta) \tag{10}$$

- ξ is the parameter vector at the η^{th} iteration
- J is the number of the items in the model for recovering the test signal (much less than the total number of sensors as the network is sparse)

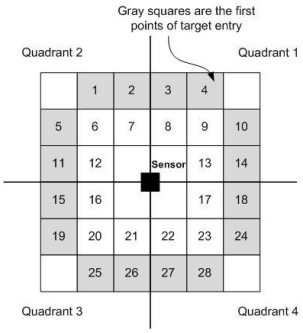

Figure 3. Sensor sensing region discretization.

- Finally, C_j is the j^{th} element of the coefficient vector C, which is generated as follows:

1- Initialize the index ($\eta = 0$).
2- Set residual signal (r) equal to the tested signal
3- Set the loop index (t) equal 1 ($t = 1$).
4- Determine the dictionary item having the largest orthogonal projection on the residual signal (r).
5- Compute the following MSE

$$\min \left\| S - \sum_{j=1}^{t} c(\eta_j)\hat{S}(\eta_j) \right\|_2 \tag{11}$$

6- Update the residual signal by subtracting the signal components found in step 5

$$\mathbf{r}_j \to \gamma - \sum_{j=1}^{t} C(\eta_j)\tilde{\gamma}(\eta_j) \tag{12}$$

7- Increment the loop index ($t = t + 1$)
8- If stopping criteria not satisfied go to step 4; else stop. Various kinds of stopping criteria are possible for the OMP algorithm; for example, number of targets found, or an error below a predefined threshold.

B. Creating a dictionary for OMP

To create the dictionary necessary for OMP, the network area was sectioned into 36 square cells of equal size. From [8], our targets have slightly different sensing regions, however, the region around each sensor with inner and outer boundaries at 10cm and 30cm is safely within the sensing regions for all targets. By paying attention to these limitations, 28 cells were selected as target points for OMP algorithm (Figure 3). Initially, given a certain target two separate magnetic field measurements were recorded for the following situations for each point:

- Measuring the ambient field when there is no target at that point (for cell i → B_{xAi} and B_{yAi}).
- Measuring the field when there is the specific target at that point (for cell i → B_{xTi} and B_{yTi}).

The difference between these values for each axis shows the effect of the target at that test point on the sensor on that axis.

$$\Delta B_{xi} = \Delta B_{xTi} - \Delta B_{xAi} \tag{13}$$

$$\Delta B_{yi} = \Delta B_{yTi} - \Delta B_{yAi} \tag{14}$$

The value of the eq.13 and eq.14 are i^{th} row of the dictionary for OMP. i^{th} row is named φ_i.

$$\boldsymbol{\varphi}_i = \left[\Delta Bx_i \quad \Delta By_i\right] \tag{15}$$

By considering these explanations the dictionary for OMP can be defined as follows:

$$\mathrm{D} = \left[\phi_1 \quad \cdots \quad \phi_i \quad \cdots \quad \phi_I\right]^T \tag{16}$$

I is the number of the test point. For this case I = 28.

C. Target identification and OMP algorithm

Identifying the target (matching it to one of the known target profiles, of which, in our testbed, there are four) and then using the related dictionary during the tracking is an important step for DISL system. A target is first identified when it breaches the outer border of the sensor coverage, and this information is used to define which target dictionary will be used in tracking phase. Identification performance based on target entry point is considered next. The position of the sensor was selected to be the center of a square with the area of $3600cm^2$. In order to create a dictionary for identification, the sensing region of a sensor was quantized to equal cells (Figure 3) (to 36 square cells and 4 square cells). In the first case, the cells which are on the border of the sensing region were selected and in second one all of the four cells were selected as target position for generating the identification dictionary. In the following equation n is the number of cells and N is number of the targets. For this case n = 16 or 4 and N = 4.

$$\mathrm{D} = \left[\phi_{1,1} \quad \cdots \quad \phi_{1,n} \quad \cdots \quad \phi_{N,1} \quad \cdots \quad \phi_{N,n}\right]^T \tag{17}$$

D. Target localization and OMP algorithm

For creating a localization dictionary, firstly the ambient magnetic field of the sensor region is measured when there was no ferromagnetic object in that region. Then target is placed in the cell number i and again magnetic field of the sensor region is measured. The difference between two measurements shows the magnetic effect of that target from cell number i on intended sensor. This value was selected as an entry for row number i of the localization dictionary. These tasks are repeated for all of the cells. As in each measurement we collect data from X and Y axes, there are two entries in each row of the localization dictionary. This dictionary will be used by OMP algorithm. During the experiments the OMP algorithm compares the measured data (eq.13 and eq.14) with an entry of the localization dictionary. The row number of dictionary which has minimum distance

with measured signal will be announced. This number shows the location of the target (cell number). Target localization is considered in three cases. More details and results are provided in part B of following section.

V. RESULTS

A. Identification

The outer perimeter of the network is discretized to 16 cells. When a specific cell is set as a known entrance point (i.e., targets are known to always enter the network from this cell) the DISL system can identify the target exactly (essential1y 100% of the time). If entrance gateway of the targets expanded to being one of among 4 cells in one quarter of the sensing region, the targets are correctly identified at a rate of 72%. If a specific cell from within each quarter is selected as an entry point, target identification can be accomplished at a rate of 67%. In the case when there is no a priori information on the potential entry point, target identification is accomplished at a rate of 48%. This is only the case when the target first enters the coverage area of the WNS. Therefore, as the target moves from one sensors coverage area to another, prior measurements can be used to gain information about potential entry points to subsequent sensing regions.

B. Localization

If the sensing region of the sensor is discretized to 28 cells with an area of 10cm × 10cm, target localization was successfully accomplished at a rate of 72%. If the location resolution is reduced to that of quadrature information, i.e. determining which quadrant about the sensor the target is positioned, then localization performance improves to 98%. This means that magnetic sensors can be used in a greater capacity than just proximity sensing. Information about quadrature positioning and direction of motion can be used in intelligent tracking and energy management algorithms to optimize sleep state management and minimize energy consumption.

VI. PRACTICAL ISSUES

In the practical implementation, important issues involving the operation of the magnetic sensors arose that were critical to ensuring the correct operation of the WSN. These issues involved the effect of daytime temperature variations, the sunset, power supply variations, and noise on sensor measurements. Experiments were conducted to quantify the impact of these real-world effects as well as impact on proposed localization and identification algorithms.

A. Temperature Variations and the Ambient Magnetic Field

A sensor was located in cardboard box with a removable cap under the sunlight. For 15 minutes the box was covered. After that the cap was removed and the sensor was under the direct sunlight. By comparing the obtained data during this test period the effect of the temperature variations on measurements was concluded.

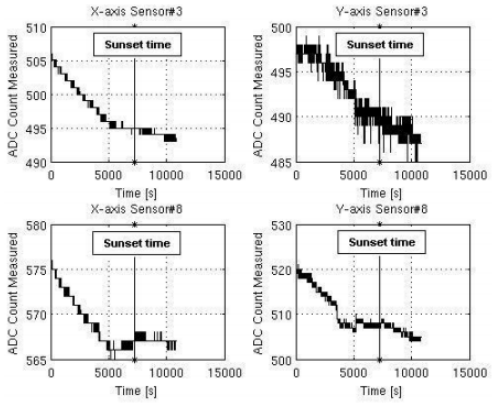

Figure 4. Sensor measurements during sunset.

TABLE I. EFFECT OF VOLTAGE VARIATION ON MEASUREMENTS

Voltage	$B_{xAmb.}$	$B_{yAmb.}$	$B_{xTar.}$	$B_{yTar.}$
3V	581	569	591	664
2.8V	572	579	583	66
2.7V	567	481	579	575

B. Sunset and the Ambient Magnetic Field

The measurements of two different sensors located at distant positions within the lab were recorded over a three hour period between 5:30pm and 8:30pm, where the sunset occurred at approximately 7:43 pm. The results of this experiment are shown in Figure 4.

C. Effect of Power Supply Variations

Table I. demonstrates the effect of the Power Supply voltage level on ADC values.

D. Effect of Magnetic Noise

Any natural variations in the earth's ambient magnetic field or magnetic field changes caused by passing vehicles, or the presence of electronic instruments may result in magnetic noise. It was observed that the motion of vehicles in the neighboring parking lot has effect on measurements

VII. CONCLUSION

This paper reports the results of a novel experimental testbed combining localization and identification of ferromagnetic targets sensed by a magnetic WSN, built to primarily understand the sensing resolution of such devices and their use in a combined localization, identification, and further, tracking network. Firstly, we have learned that localization with a single sensor can be accomplished to yield information beyond just that of a target being located within the vicinity of the sensor. More specifically, sequential localization yielding both quadrant and location within a

10 cm x 10 cm square is possible. Secondly, using the OMP algorithm, we can successfully discriminate between four predefined ferromagnetic targets that are rather similar in size and properties. However, we have also understood that there are some practical issues that impact network performance to a point that they need to be taken into account when designing or simulating the network: temperature variations turned out to be critical for sensor performance thus the performance of the overall system. Also critical are variations in power supply- therefore, keeping battery levels more or less constant (perhaps through ambient energy harvesting or other recharging mechanisms) is important for this type of WSN. Finally, eliminating magnetic noise (or calibrating sensors accordingly), estimating sensor sensitivity well, and knowing sensor axis orientations were found to be immensely important. This work provides guidelines as to how to model the capabilities and limitations of magnetic sensor nodes as components of a sparse WSN. Future work can exploit this knowledge to construct simulations of larger networks of such components using models of these components. One goal is to further develop the algorithms to incorporate Kalman Filter-based tracking algorithms. The multi-target case may then be further investigated in the situation of multiple targets appearing in the sensing area of the same node simultaneously.

ACKNOWLEDGMENT

This work was supported in part by the Scientific and Technological Research Council of Turkey (TUBITAK) Project No. 110E252 and the EU FP7 Project No. PIRG-GA-2012-268276.

REFERENCES

[1] R Dhar A., Kulkarni P., Using magnetic sensors to estimate street traffic patterns (www.cse.iitb.ac.in).

[2] Cheung S.Y., Coleri S., Dundar B., Ganesh S., Tan C., Varaiya P., Traffic Measurment and Vehicle Classification with a Single Magnetic Sensor, UC Berkeley, PATH paper, 2004.

[3] Lee S., Yoon D., Ghosh A., Intelligent parking lot application using wireless sensor networks, Int. Symp. on Collaborative Technologies and Systems (CTS), 19-23 May 2008, sf. 48-57.

[4] Boda V.K., Nasipuri A., Howitt I., Design consideration for a wireless sensor network for locating parking spaces, in Proc. SoutheastCon, 2007.

[5] Cheung S.Y., Ergen S.C., Varaiya P., Traffic surveillance with wireless magnetic sensors, U.C. Berkeley, California PATH Research Report, 2007.

[6] Kaewkamnerd S., Chinrungrueng J., Pongthornseri R., Song-phon Dumnin, "Vehicle classification based on magnetic sensor signal," Int. Conf. on Inf. and Automation (ICIA), 20-23 June 2010, sf.935-939.

[7] Dimitropoulos K., et. al., Detection, tracking and classification of vehicles and aircraft based on magnetic sensing technology, Trans. Eng. Computing and Tech., Vol. 14, 2006, sf. 161-166.

[8] Antepli M.A., Gurbuz S.Z., Uysal-Biyikoglu E., Ferromagnetic target detection and localization with a wireless sensor net-work, MILCOM 2010.

[9] Wikipedia. Simulated annealing. (Last visited on May 2012). www.en.wikipedia:org_wiki_Simulatedannealing.

[10] Pati Y.C., Rezaiifar R., Krishnaprasad P.S., Orthogonal match-ing pursuit: Recursive function approximation with applica-tions to wavelet decomposition, in Proc. of the 27 th Asilomar Conference on Signals, Systems, and Computing, 1993.

[11] Tropp J.A., Gilbert A.C., "Signal recovery from random measurements via orthogonal matching pursuit," Trans. Info. Theory, Vol.53, No.12, Aralk 2007, sf. 4655-4666.

[12] Cai T.T., Wang L., Orthogonal matching pursuit for sparse signal recovery with noise, Trans. Information Theory, Vol.57, No.7, Temmuz 2011, sf. 4680-4688.

[13] Gurbuz S.Z., Melvin W.L., Williams D.B., Radar-based human detection via orthogonal matching pursuit, ICASSP, 2010.

[14] Gurbuz A.C., Scott W.R., McClellan J.H., "Location estima-tion using a broadband electromagnetic induction array", Proc. SPIE, Vol. 7303, 2009.

[15] Anastasi G., Conti M., Di FrancescoM., Passarella A., Energy conservation in wireless sensor networks: A survey, Ad Hoc Networks, Vol. 7, Iss. 3, May 2009, pp. 537-568.

[16] Raghunathan V., Schurgers C., Park S., Srivastava M.B., Energy-aware wireless microsensor networks, IEEE Signal Processing Magazine, Vol. 19, Iss. 2, March 2002, pp. 40-50.

[17] Xing G., Sha M., Hac kmann G., Klues K., Chipara O., Lu C., Towards unified radio power management for wireless sensor networks, Wirel. Commun. Mob.Comput., Vol 9, No. 3, March 2009.

[18] Sinha A., Chandrakasan A., Dynamic power management in wireless sensor networks, IEEE Design and Test of Computers, Vol. 18, Iss. 2, Mar/Apr 2001, pp. 62-74.

[19] Crossbow, MTS/MDA Sensor Board Users Manual, Revision A., June 2007, www.xbow.com..

[20] Honeywell Magnetic Sensors Product Data Sheet, 1- and 2-Axis Magnetic Sensors, Honeywell SSEC, 2004, www.honeywell.com.

[21] Ctp: collection tree protocol. [Online]. Available (Last visited on May 2012): www.sing.stanford.edu/pubs/sing-09-01.pdf.

[22] TinyOS. (Last visited on May 2012).

[23] Griffiths D.J., Introduction to Electrodynamics. Prentice Hall, 1999.

[24] Arora A., et. al., A line in the sand: A wireless sensor network for target detection, classification, tracking, Computer Networks, Vol. 46, No. 5, 2004, pp. 605-634.

[25] TinyOS. (Last visited on May 2012) www.tinyos.net/tinyos-2.x/doc/html/tep118.html.

[26] Baghaee S. , Identification and Localization on a Wireless Magnetic Sensor Network. M.Sc. thesis, Middle East Technical University, Turkey, 2012.

[27] INA126 INA2126 Micropower Instrumentation Amplifier Single and Dual Versions, Burr-Brown, 1996.

[28] Wikipedia. Basis pursuit.(Last visited on May 2012). www.en.wikipedia.org/wiki/Basispursuit..

[29] Wikipedia. Matching pursuit.(Last visited on May 2012). www.en.wikipedia.org/wiki/Matchingpursuit.